

# Field-enhanced diamagnetism in intense magnetic field in the pseudogap state of the cuprate $\text{Bi}_2\text{Sr}_2\text{CaCu}_2\text{O}_{8+x}$

Yayu Wang<sup>1</sup>, Lu Li<sup>1</sup>, M. J. Naughton<sup>2</sup>, G. D. Gu<sup>3</sup>, S. Uchida<sup>4</sup>, N. P. Ong<sup>1</sup>

<sup>1</sup>Department of Physics, Princeton University, New Jersey 08544, U.S.A.

<sup>2</sup>Department of Physics, Boston College, Chestnut Hill, Massachusetts 02467, U.S.A.

<sup>3</sup>Department of Physics, Brookhaven National Laboratory, Upton, N.Y. 11973.

<sup>4</sup>School of Frontier Science, University of Tokyo, Tokyo 113-8656, Japan.

(Dated: February 8, 2020)

In hole-doped cuprates, Nernst experiments imply that the superconducting state is destroyed by spontaneous creation of vortices which destroy phase coherence. Using torque magnetometry on  $\text{Bi}_2\text{Sr}_2\text{CaCu}_2\text{O}_{8+x}$ , we uncover a field-enhanced diamagnetic signal  $M$  above the transition temperature  $T_c$  that increases with applied field to 32 Tesla and scales just like the Nernst signal. The magnetization results above  $T_c$  distinguish  $M$  from conventional amplitude fluctuations, and strongly support the vortex scenario for the loss of phase coherence at  $T_c$ .

PACS numbers: 74.25.Dw, 74.72.Hs, 74.25.Ha

In bulk superconductors, the superconducting transition involves vanishing of the macroscopic wave function  $\psi$ , but in hole-doped cuprates there is growing evidence that the transition is caused by the proliferation of vortices which destroy long-range phase coherence. The detection of a large Nernst signal  $e_N$  and kinetic inductance above the critical transition temperature  $T_c$  has provided evidence for the vortex scenario [1, 2, 3, 4, 5, 6]. However, the magnetization evidence is ambiguous. Using high-field, high-resolution torque magnetometry on  $\text{Bi}_2\text{Sr}_2\text{CaCu}_2\text{O}_{8+x}$  (Bi2212), we show the existence of a field-enhanced diamagnetism above  $T_c$  that closely matches the Nernst signal as a function of both field  $H$  and temperature  $T$ . In addition to establishing the unusual nature of the transition and its diamagnetic state above  $T_c$ , our results clarify the unusual behavior of the upper critical field  $H_{c2}(T)$ .

In the vortex scenario, the long-range phase coherence, essential for superfluidity, is destroyed by mobile vortices. Despite the loss of phase coherence above  $T_c$ , we should expect a magnetization  $M$  that differs qualitatively from 'fluctuation diamagnetism' observed in low- $T_c$  superconductors. Further, the magnetization should reveal a depairing field scale that remains very large at  $T_c$  [analogous to the Kosterlitz-Thouless (KT) transition [7]].

We have performed detailed high-field torque magnetometry on single crystals of underdoped (UD), optimally-doped (OP) and overdoped (OD) Bi2212. The crystal is glued to the tip of a Si cantilever with its  $c$ -axis at an angle  $\theta_0 = 15^\circ$  to  $H$  (Fig. 1a, inset). The torque  $\tau = m \times B$  leads to a flexing of the cantilever which is detected capacitively, where  $m$  is the sample's magnetic moment and  $B = \mu_0(H + M)$  with  $\mu_0$  the vacuum permeability. We resolve  $m = 5 \times 10^9$  emu at 10 T. Measurements were also performed in a SQUID magnetometer (with resolution  $10^6$  emu). All curves of  $M$  reported here are fully reversible in  $H$  and  $T$ . Torque magnetometry has been applied to cuprates previously [8, 9, 10]. However, the high-field results, especially the scaling with the Nernst signal, point to conclu-

sions very different from earlier studies.

The torque curves measured in an underdoped (UD) Bi2212 crystal, with  $T_c = 50$  K, are shown in Fig. 1a. Above 120 K, is dominated by a paramagnetic term that changes little from 200 to 120 K. Below 120 K, however, a diamagnetic term appears, and grows rapidly to pull the torque to large negative values. The maximum deflection angle of the cantilever is  $10^{-2}$  rad.

We express [8] the torque as an effective magnetization  $M_{\text{eff}} = B \chi V$ , with  $V$  the sample volume and  $B_x = B \sin \theta_0$  (we take  $\theta_0 = 15^\circ$ ). For  $\theta_0 = 1$ , we may show that  $M_{\text{eff}} = \chi_p H_z + M(T; H_z)$  where the spin susceptibility anisotropy  $\chi_p = \chi_c - \chi_a$  is the difference between the  $c$ -axis and in-plane spin susceptibilities, and  $M(T; H_z)$  is the magnetization of interest here. A crucial finding [11] is that  $\chi_p$  in cuprates has a weak  $T$  dependence. In  $\text{La}_{2-x}\text{Sr}_x\text{CuO}_4$  (LSCO) with  $x = 0.050$ , in which  $T_c < 2$  K and  $M(T)$  is not resolved above 25 K,  $M_{\text{eff}}(T) = \chi_p H_z$  changes by only 6% between 200 and 25 K (open circles in Fig. 1b). Likewise, in both Bi2212 samples,  $M_{\text{eff}}(T) = \chi_p H_z$  shows a weak  $T$  dependence from 200 K to 120 K (solid symbols). Starting at 120 K, the steep growth of  $M(T)$  causes  $M_{\text{eff}}(T)$  to deviate downwards from its high- $T$  trend. In view of its weak  $T$  dependence, we may extrapolate  $\chi_p$  as a straight line below 120 K. We identify  $M(T; H)$  as the difference between this line and  $M_{\text{eff}}(T)$  (shaded areas in Fig. 1b). Hereafter, we discuss  $M(T; H)$  only and write  $H_z$  as  $H$ .

Figure 2 compares the  $M(T; H)$  vs.  $H$  curves in the UD and OP samples. In the UD sample [Panel (a)], a large diamagnetic signal appears at 120 K and grows over a broad 70-K interval as  $T \rightarrow T_c$  (bold curve). As  $T$  falls below  $T_c$ , rapid changes caused by the growth of the Meissner signal become apparent in low  $H$ . The curves in Fig. 2b behave in a similar way except that the interval above  $T_c$  with enhanced diamagnetism is narrower (30 K). The  $T$  dependences of the magnetization in fixed  $H$  are displayed in Figs. 2c and 2d for fields up to 32 T. Previously, low-field experiments [12, 13] suggested that all curves of  $M$  vs.  $T$  intersect at a single crossing

temperature'. We focus instead on the robustness of the signal up to 32 T over a broad interval of  $T$  above  $T_c$ .

At first glance, the curves in Fig. 2 recall the well-known \textit{fluctuation diamagnetism}  $M^0$  in low- $T_c$  type II superconductors which are produced by amplitude fluctuations  $\hat{j}_j$  [14, 15]. Previous diamagnetism in cuprates measured above  $T_c$  (to lower  $H$ ) was interpreted as amplitude fluctuations [19] or not conclusively identified [8, 9, 10, 13].

We now show that the diamagnetism in Bi2212 is actually qualitatively distinct from amplitude fluctuations. The evidence are of 3 types. First, we focus on  $T > T_c$ . As seen in Fig. 2, in a field of 32 T,  $M$  survives as a long tail over a 70-K interval (30-K interval) above  $T_c$  in the UD (OP) sample. This robustness in intense fields sharply distinguishes the cuprate signal from that in low- $T_c$  superconductors. To emphasize this important difference, we focus on the OP sample (Fig. 2d). With  $H = 10$  Oe,  $M$  displays a sharp Meissner transition at  $T_c = 87$  K. However, a field of 3 T \textit{amplifies} the diamagnetic signal by 3 orders of magnitude rendering  $M$  observable to 104 K. Further increase of  $H$  to 32 T makes the signal visible to 120 K. The monotonic increase of  $M$  with  $H$  implies that the condensate is not destroyed in a 32-Tesla field, i.e. the depairing field  $H_{c2}$  lies significantly higher at these  $T$ . In the UD sample (Fig. 2c), a phase of volume 2.5% (estimated from ) with higher  $T_c \sim 70$  K is apparent as a \textit{foot} extending from 50 to 70 K. As discussed below, this small phase does not affect our conclusions.

By contrast, in low- $T_c$  superconductors, the fluctuation signal  $M^0$  from amplitude fluctuations is suppressed in weak  $H$ . In Nb,  $M^0$  becomes unresolved above 1000 Oe (see Fig. 13 of Ref. [15] for curves for Nb, In and Pb and alloys). There the field sensitivity reflects the approach  $H_{c2}(T) \rightarrow 0$  at  $T_c$ , and the role of nonlocal electrodynamics in suppressing short-wavelength fluctuations [25].

Secondly, we show that the diamagnetic signal above  $T_c$  is closely related to the Nernst signal (measured in the same crystals). In Figs. 3a and 3b, we plot the  $T$  dependence of  $e_N$  and  $M$  (both at 14 T) in the UD and OP samples, respectively (the 10-Oe curves are shown as dashed curves). Remarkably,  $M$  (solid circles) tracks  $e_N$  (open) over a broad interval of temperature before diverging near  $T_c$ . Below  $T_c$ ,  $M$  rises steeply whereas  $e_N$  attains a broad peak before decreasing towards zero (its value in the vortex solid phase). The 2 signals  $M$  and  $e_N$  share the same onset temperature  $T_{\text{onset}}$ .

In both samples, the direct proportionality between  $M$  and  $e_N$  above  $T_c$  also holds as  $H$  is varied. We compare their respective field profiles in the UD sample in Fig. 3c. Over the interval 70–120 K, we find that the  $M$  vs.  $H$  curves (solid) can be overlaid on the  $e_N$  vs.  $H$  curves (dashed) with the same scaling factor as in Fig. 3a. (Figure 3c also clarifies the contribution of the minority phase in the UD sample. At 60 and 65 K, the 2.5% phase adds a small term to  $M$  that is nearly constant

in  $H$ . However, it does not contribute to  $e_N$  because it does not extend over the sample, so the curves of  $M$  lie slightly above  $e_N$  below 70 K. Above 70 K, this difference is unobservable. The 2.5% phase cannot account for the large diamagnetic signal extending to 120 K.) In terms of the resistivity  $\rho_{xx}$  and  $\rho_{xy}$ , we have  $e_N = \rho_{xy}$  [the quantity  $\rho_{xy}$  relates the transverse charge current  $J_y$  to the gradient, viz.  $J_y = \rho_{yx} (\partial_x T)$ ]. The scaling relationship is then  $\rho_{xy} = M$  for  $T > T_c$ : The linear relationship between  $M$  and  $\rho_{xy}$  close to  $H_{c2}$  was calculated by Caroli and Maki [20], and later corrected for the magnetization current [21, 22]. Figure 3 confirms that, above  $T_c$ , the growth of  $e_N$  is accompanied by an increase in the strength of the screening diamagnetic current as required by the vortex scenario.

Lastly, we describe the behavior of  $H_{c2}(T)$  inferred from the curves at  $T < T_c$  (Fig. 4a). In type II superconductors, the linear decrease of  $M(H)$  to zero, viz.  $M \propto [H_{c2}(T) - H]$ , provides a reliable way to determine  $H_{c2}(T)$ . In Fig. 4b we plot  $M$  in NbSe<sub>2</sub> (measured by SQUID magnetometry) against  $\log H$ . The values of  $H_{c2}(T)$  so determined approach zero linearly in the reduced temperature  $t = 1 - T/T_c$  as  $T \rightarrow T_c$  (to logarithmic accuracy  $H_{c2}(T)$  may be estimated by linear extrapolation of  $M \propto \log H$  to the  $H$ -axis). As noted, the vanishing of  $H_{c2}(T)$  causes the amplitude fluctuations to be sensitive to field.

The curves of  $H_{c2}(T)$  in Bi2212 behave in a qualitatively different way. Figure 4a plots the curves of  $M$  vs.  $\log H$  in the OP sample from 0.4 T to 32 T at temperatures 35 to 91 K. At each  $T$ , the decrease in  $M$  is nominally linear in  $\log H$ , but  $M$  clearly retains significant strength at 32 T. Instead of going to zero,  $H_{c2}(T)$  remains high above 32 T as  $T \rightarrow T_c$ , consistent with the  $H_{c2}$  behavior inferred from  $e_N$  [3, 4]. The contrast with low- $T_c$  superconductors is striking.

If we assume that  $M$  remains nominally linear in  $\log H$  above 32 T (as the curves for NbSe<sub>2</sub> suggest), we may estimate  $H_{c2}$  with logarithmic accuracy. The broken lines imply that  $H_{c2}$  decreases from 200 T to 90 T between 35 K and 85 K. The value at 85 K is nominally similar to the estimate from  $e_N$  in Ref. [4].

Taken together, the evidence suggest that the depairing field  $H_{c2}$  remains at 90 T as  $T$  crosses  $T_c$ . Hence, above the melting line  $H_m(T)$ , the amplitude  $\hat{j}_j$  is finite beyond our highest field 32 T, but the phase is strongly disordered. The vortex-liquid state starts at  $H_m(T)$  (for  $T < T_c$ ) and continues smoothly to  $T_{\text{onset}}$ . The present results establish an essential link between the magnetization and the Nernst experiments above  $T_c$ . In equilibrium in  $H$ , local screening supercurrents in the vortex liquid are observed as a robust diamagnetic signal, while in an applied gradient  $\nabla T$  the flow of vortices leads to a large Nernst signal proportional to  $M$ . In zero field, the collapse of the Meissner effect at  $T_c$  arises from the spontaneous creation of vortices which destroy long-range phase coherence [23]. The robustness of  $M$  to intense fields for  $T > T_c$  provides a key experimental signature for the

unusual nature of the transition. Finally, the observation of a depairing field that remains very large at  $T_c$  is crucial for the vortex dephasing scenario (the KT case is discussed in Refs. [7, 24]).

As shown in Fig. 4c,  $T_{\text{onset}}$  lies significantly below the pseudogap temperature  $T^*$  determined from spectroscopy [25]. The extension of the vortex-liquid state above  $T_c$  in Fig. 3c implies a close relationship between the pseudogap state and d-wave superconductivity. It suggests that Cooper pairing with a large binding energy already exists over the lower half of the pseudogap state, but long-range phase coherence only occurs at  $T_c$ . The

origin of the enhanced  $M$  and  $e_N$  is deeply entwined with the physics of spin-singlet formation and the spin-gap [25] that opens at  $T^*$  higher than  $T_{\text{onset}}$ .

We thank P. A. Lee, S. Sondhi, V. Oganesyan and I. Ussishkin for helpful comments. High-field measurements were performed at the National High Magnetic Field Laboratory, Tallahassee, which is supported by the U.S. National Science Foundation (NSF) and the State of Florida. This research is supported by NSF Grant DMR-0213706. GDG was supported by the DOE under contract No. DE-AC02-98CH10886.

- 
- [1] Z. A. Xu, N. P. Ong, Y. Wang, T. Kakeshita, S. Uchida, *Nature* 406, 486 (2000).
  - [2] Yayu Wang et al., *Phys. Rev. B* 64, 224519 (2001).
  - [3] Yayu Wang et al., *Phys. Rev. Lett.* 88, 257003 (2002).
  - [4] Yayu Wang et al., *Science*, 299, 86 (2003).
  - [5] N. P. Ong and Yayu Wang, *Physica C* 408, 11-14 (2004).
  - [6] J. Corson, R. M.allozzi, J. Orenstein, J. N. Eckstein, and I. Bozovic, *Nature* 398, 221 (1999).
  - [7] S. Doniach and B. A. Huberman, *Phys. Rev. Lett.* 42, 1169 (1979);
  - [8] C. Bergemann et al., *Phys. Rev. B* 57, 14387 (1998).
  - [9] M. J. Naughton, *Phys. Rev. B* 61, 1605 (2000).
  - [10] J. Hoffer et al., *Phys. Rev. B* 62, 631 (2000).
  - [11] Lu Li, Yayu Wang and N. P. Ong et al., unpublished.
  - [12] P. Kes et al., *Phys. Rev. Lett.* 67, 2383 (1991).
  - [13] U. Welp et al., *Phys. Rev. Lett.* 67, 3180 (1991).
  - [14] R. P range, *Phys. Rev. B* 1, 2349 (1970).
  - [15] J. P. Gollub, M. R. Beasley, R. Callarotti, and M. Tinkham, *Phys. Rev. B* 7, 3039 (1973).
  - [25] P. A. Lee and M. G. Payne, *Phys. Rev. Lett.* 26, 1537 (1971).
  - [17] Q. Li et al., *Phys. Rev. B* 48, 9877 (1993).
  - [18] V. G. Kogan et al., *Phys. Rev. Lett.* 70, 1870 (1993).
  - [19] C. Carballera, J. Mosqueira, R. Revcolevschi, and F. Vidal, *Phys. Rev. Lett.* 84, 3517 (2000).
  - [20] C. Caroli, and K. Maki, *Phys. Rev.* 164, 591 (1967).
  - [21] C. R. Hu, *Phys. Rev. B* 13, 4780 (1976).
  - [22] I. Ussishkin and S. L. Sondhi, *cond-mat/0406347*.
  - [23] V. J. Emery and S. A. Kivelson, *Nature* 374, 434 (1995).
  - [24] V. Oganesyan, D. A. Huse and S. L. Sondhi, *cond-mat/0502224*.
  - [25] For a review, see P. A. Lee, N. Nagaosa, X. G. Wen, *cond-mat/0410445*.

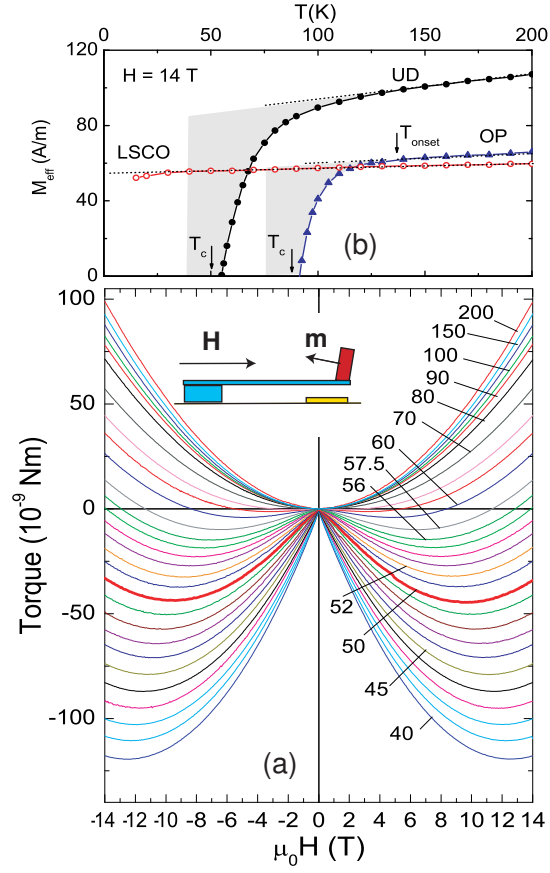


FIG. 1: (a) The measured torque vs.  $H$  at selected  $T$  in UD Bi2212 with  $T_c = 50$  K (crystal size  $0.2 \times 1 \times 1$  mm<sup>3</sup>). The parabolic behavior above 120 K arises from the anisotropy term  $\mu_p H_z$ . Below 120 K, a diamagnetic contribution  $M$  grows rapidly. Measurements were extended to 32 T at selected  $T$ . The inset shows the Si cantilever and the magnetic moment  $m$  of the crystal. The maximum beam deflection is  $0.15^\circ$ . (b) The  $T$  dependence of  $M_{eff}$  in single-crystal UD and OP Bi2212 (solid symbols) and in LSCO ( $x = 0.050$ , open circles) at  $B = 14$  T. The LSCO data show that  $\mu_p$  is only weakly  $T$ -dependent down to 25 K. In Bi2212, the diamagnetic signal  $M(H_z)$  is shown shaded.

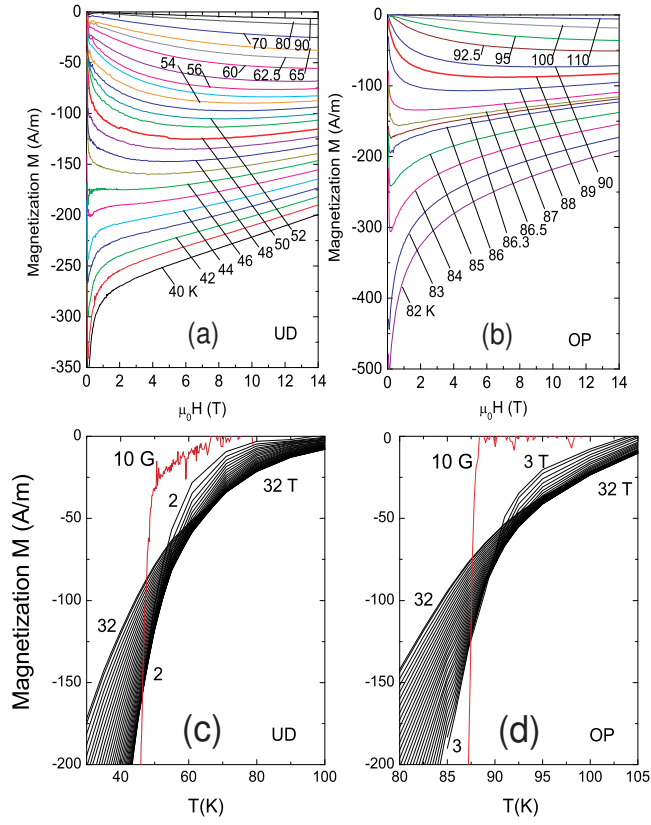


FIG. 2: Curves of magnetization  $M(T; H)$  plotted vs.  $H$  at selected  $T$  in the (Panels a and b), and plotted vs.  $T$  in (c and d) for the UD ( $T_c = 50$  K) and OP ( $T_c = 87$  K) samples. In (a) and (b), the bold curve is taken at  $T_c$ . In Panels (c) and (d), the  $T$  dependence of  $M$  is plotted at fixed  $H$  in the UD and OP sample, respectively [ $H$  decreases, in steps of 1 Tesla, from 32 T to 2 T in (a) and 3 T in (b)]. Curves labelled 10 G show the Meissner transition at  $T_c$  measured at  $H = 10$  Oe. In the UD sample, the foot above 50 K is a minority phase 2.5% in volume (see text). Increasing  $H$  to values 3–32 T greatly amplifies the diamagnetic signal in a broad interval above  $T_c$ .

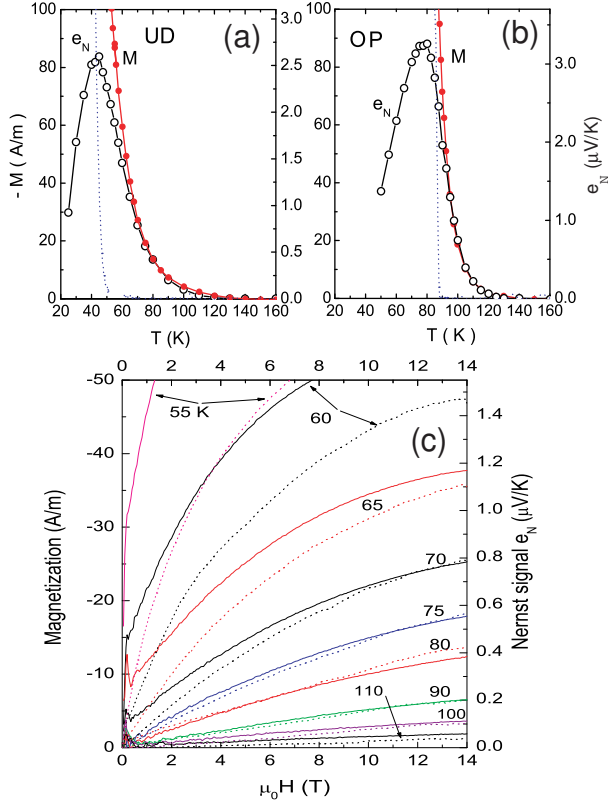


FIG. 3: Comparison of  $M$  and the vortex-Nemst signal  $e_N$  measured at 14 T in the UD (Panel a) and OP (b) Bi2212, and comparison of their field profiles in UD Bi2212 (Panel c). In Panels (a) and (b),  $M$  and  $e_N$  track each other at high  $T$ . Below  $T_c$ ,  $M$  increases rapidly while  $e_N$  attains a peak before falling towards zero in the vortex-solid phase. The dashed curves show  $M$  measured in  $H = 10$  Oe. Panel (c) shows that curves of  $M$  vs.  $H$  (solid curves) match those of  $e_N$  vs.  $H$  (dashed curves) in the UD sample above  $T_c$  (the scale factor between  $M$  and  $e_N$  is the same as in Panel a). The observed Nemst signal is the sum of the vortex contribution and a negative, quasiparticle (qp) term  $e_N^{\text{obs}} = e_N + e_N^{\text{qp}}$ . The curves show  $e_N$  after the small qp term is subtracted ( $e_N^{\text{qp}} < 0.04$  V/K).

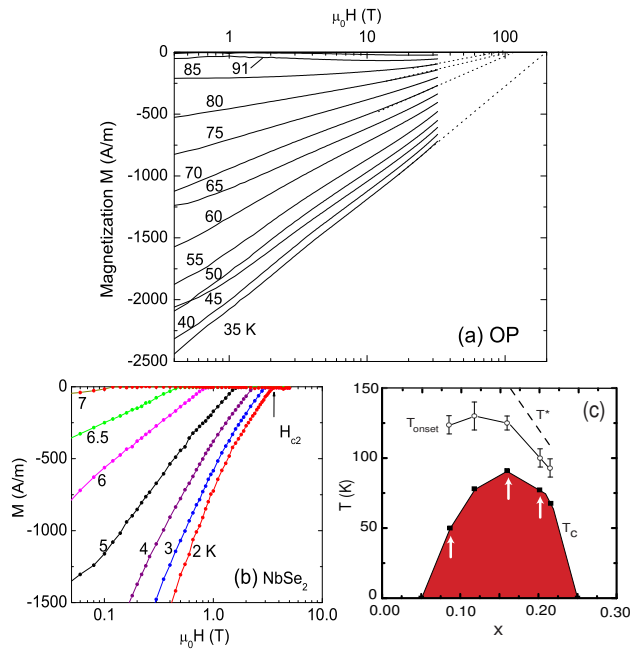


FIG. 4: Plot of the field dependence of  $M$  in OP Bi2212 (Panel a) and in NbSe<sub>2</sub> (b) and the phase diagram of Bi2212 (Panel c). In Panel a, the measured  $M$  extends from 0.4 to 32 T at temperatures 35 K to 91 K. Normally,  $M$  decreases linearly with  $\log H$ . The  $H_{c2}(T)$  values estimated by extrapolation (broken lines) remain at above 90 T as  $T \rightarrow T_c$  (86 K). In Panel b, the measured  $M$  also shows a normally linear dependence on  $\log H$ . However, in contrast with (a),  $H_{c2}(T)$  decreases from 3.6 T to 0.12 T as  $T$  rises from 2 to 7 K. In Panel c,  $T_{onset}$  of both  $M$  and  $e_N$  is plotted vs.  $x$  (hole content) together with  $T_c$  and  $T^*$ . Arrows indicate the 3 samples studied by torque magnetometry.